Structural and Phase Transition Temperature Study of Some Iron Rich Soft Ferromagnetic Materials

Debashis Das

Department of Physics, Shibpur Dinobundhoo Institution (College)

DOI: https://doi.org/10.51584/IJRIAS.2026.11050188

Received: 17 May 2026; Accepted: 22 May 2026; Published: 13 June 2026

ABSTRACT

There are huge varieties of soft magnetic alloys having widespread applications in variety aspects of science and technology. However, in this paper we will discuss the X-Ray diffraction pattern of the samples FINEMET ($Fe_{73.5}Nb_3Cu_1Si_{13.5}B_9$), SAMPLE-1 ($Fe_{81}B_{12}Mo_7$), SAMPLE-2 ($Fe_{80}B_{12}Mo_7Cu_1$), SAMPLE-3($Fe_{82}B_{12}Mo_7Cu_1$) & SAMPLE-4($Fe_{83}B_{12}Mo_5$). The peak intensity (~ 0.16 a.u.) for the amorphous metal is extremely small compared to that for a crystalline substance where the peak intensity ranges up to some thousand a.u. The XRD pattern resembles that the samples are fully amorphous material. We have also Study of the paramagnetic transition temperature of the S1($Fe_{81}B_{12}Mo_7$), S2($Fe_{80}B_{12}Mo_7Cu_1$), samples. These samples are magnetically soft materials.

Keywords- Soft ferromagnetic materials, scattered ray, Bragg's law, polycrystalline specimen, XRD. Currie temperature.

PRESENT STUDY

When the wavelength of X-rays incident on a crystal is of the order of the inter-atomic distance in the crystal, the x-rays are diffracted. Diffraction is essentially due to the existence of certain phase relations between two or more waves. Consider a wave incident on a crystal. If the different planes of the crystal (A, B and C) are d distance apart then the path difference between the waves scattered from two consecutive planes would be $2d\sin\theta$, θ-being the incident angle. In order that the scattered rays, be completely in phase with each other their path difference should be integer number n of wavelengths.

$$2d\sin\theta = n\lambda$$

This is known as Bragg's law. Diffraction takes place from the crystal only when Bragg condition is fulfilled [Klug and Alexander 1974, Kittel 1996]. This condition can be achieved by continuously changing either **λ** or **θ** during the experiment. There are mainly three experimental methods for recording X – ray diffraction.

	λ	**θ**
Laue method	variable	fixed
Rotating crystal method	fixed	variable
Debye-Scherrer powder method	fixed	variable

In the Debye-Scherrer powder method the sample to be examined is placed in the path of a beam of monochromatic X-rays. In the crystalline powder specimen various reciprocal lattice vectors are randomly oriented with respect to the incident beam and Bragg diffraction occurs over a set of cones, known as Debye - Scherrer cones. The incident monochromatic radiation strikes on a fine powdered sample or a fine-grained polycrystalline specimen contained in a sample holder. Diffracted beam goes out from the individual crystallites

ISSN No. 2454-6194 | DOI: 10.51584/IJRIAS |Volume XI Issue V May 2026

that happen to be oriented with planes making an incident angle θ with the beam satisfying the Bragg equation $2d\sin\Theta = n\lambda$. Diffracted rays leave the specimen along the generators of the cones concentric with original beam. The generators make an angle of 2Θ with the direction of the original beam, where Θ is the Bragg angle. Powder specimen is rotated in order to increase the number of planes contributing to each reflection. The sample is rotated by an angle Θ and the detector by 2Θ continuously in such a way that only the crystals whose planes are parallel to the sample surface take part in the diffraction and result in constructive interference. The advantages of this method are: (1) small amount of powder required, and (2) practically complete coverage of all the reflection produced by the specimen.

Diffraction pattern depends on the crystal structure and on the wavelength of the incident beam. One can use photons, neutrons as well as electrons for creating diffraction pattern. We have used x- ray diffraction in our work and in the following we describe this in some details.

Structural Study

The XRD pattern are recorded for the characterization of all the samples employing diffractometer using CoKα (λ = 1.541838 Å) radiation for the FINEMET sample and CuKα radiation for the rest of the samples. In the following figures we have shown a typical XRD pattern for the alloys. The scanning has been done for all the samples from 2θ = 20 to 1000 with 1.20/ min. speed (slow scan mode). The reason for taking slow scan is to investigate the possible presence of any secondary phase. The results obtained for various samples are given as follows:

Magnetism in solids is a subject, which continues to draw attention because of its technological importance. It also challenges the ingenuity of both experimental and theoretical condensed matter physicists. Magnetism is a fascinating subject by itself and has some role to play in almost every branch of science and technology. Before a few decades, "Magnetism in solids" was thought to be an orderly subject. In spite of having several disputes about the microscopic origin of different types of magnetic behaviour at that time, only five basic types of magnetic order were distinguished in the realm of magnetism. These are Diamagnetism, Para magnetism, Ferromagnetism (FM), Antiferromagnetism (AFM) and Ferromagnetism. It has been established that, apart from closed shell diamagnetism and the diamagnetism and Para magnetism of conduction electrons, magnetic behaviour comes from permanent, microscopic magnetic moments, possessed by some or all the ions in a solid.

Later on, an entirely new kind of theoretical and experimental activity involving (i) Amorphous solids, in which no two atomic sites are equivalent and (ii) disordered alloys, in which different atoms occupy randomly the sites of a regular crystal lattice, created a lot of excitement in the domain of "Magnetism in solids". The subject has since then expanded from the original five types of magnetic behaviour to many more types, namely, mictomagnetic, asperomagnetic, sperimagnetic, metamagnetic, spin glass, cluster glass, superparamagnetic, etc. Magnetic systems with competing interactions were first investigated four decades ago. Well known examples include the Ising model on the triangular lattice with AFM n.n. interactions studied by Wannier in 1950.

Helical structure was discovered in the Heisenberg model with n.n. interactions independently by Yoshimori and Villain in 1959. However, extensive investigations in magnetic systems with competing interactions have really started with the concept of frustration introduced almost at the same time by Toulouse and Villain in 1977 in the context of spin glasses.

SAMPLE PREPARATION TECHNIQUES OF PREPARATION

Preparation of Amorphous Glass materials

A number of techniques which provide cooling rates from 1 K/sec to 10^{15} K/sec have been used to produce glassy materials. The normal quenching methods used in the metallurgical industries have quenching rates of 1 to 10^3 k/sec. These are however insufficient for producing glassy or amorphous metals or metalloids and metal-metal alloys which require cooling rates of 10^6 K/sec. For this purpose, several rapid liquid quenching techniques have been developed.

ISSN No. 2454-6194 | DOI: 10.51584/IJRIAS |Volume XI Issue V May 2026

Melt Spinning

Among the most commonly used rapid liquid quenching techniques today is the melt spinning. This technique has the advantage of giving long ribbons having uniform cross-section and reproducible properties. This is the reason for its being used for large scale commercial production of amorphous alloys. A melt spinner consists of a disc, usually of copper, which is rotated at a high speed to generate a rim velocity of more than 50 $msec^{-1}$. A properly superheated molten alloy is ejected under high pressure through a fine nozzle at the bottom of a refractory tube on to the spinning disc. The alloy is melted by rf induction heating under an inert helium or argon atmosphere.

Sputtering

Besides rapid liquid quenching by melt spinning, the most widely used technique for the formation of glassy metals is sputtering. Sputtering is defined as the process by which atoms or molecular groups are released from a target (cathode) under the bombardment of positive ions.

Ion Implantation

Recently a technique called "ion implantation" has been extensively used for modifying the properties of the surface layers of thin films specially of semiconductors. In this technique high speed ions are allowed to impinge on the surface. These ions travel a short distance and get embedded within the top few atomic layers (10 nm to 1 μm) of the material. In this process the quenching rate is estimated to be about 10^{14} K/sec. It is possible to produce amorphous Para-surface layers in crystalline solids by implanting ions in high dose.

Preparation of Polycrystalline Sample

These samples were prepared by induction melting of required amount of "spec-pure" grade constituent elements. Initially the pure elements are cleaned with organic solvent HNO_3, after which the required amounts are cut and weighed carefully. A water-cooled induction furnace with a maximum power of 7 kW, fed by an "Ajax Magno thermic Converter" (which converts the line-frequency of 50 Hz to a value between 20 to 40 kHz depending on power consumption), is used for melting. The required elements are kept in a high-quality alumina crucible which is then placed in a graphite susceptor. Now the whole thing is put in a vacuum sealed quartz tube inside the furnace. The quartz tube is repeatedly evacuated to 10^{-3} Torr and flushed with high purity argon gas. Finally, it is sealed after filling the argon gas at much less than atmospheric pressure. During the heating process, an optical pyrometer is used to monitor the increase in temperature. As soon as the elements get melted, the furnace is turned off to cool the melt in the furnace. All the homogenized alloys in the bulk form are the cold rolled (30% cold work) in the form of a sheet and cut into thin rectangular strips as well as in needle forms for various transport and magnetic measurements. All the pieces are then finally annealed in argon atmosphere in a sealed quartz tube for 30 hours at 1050 ^{0}C to reduce strain in the specimen introduced due to cold work. These annealed samples are then quenched fast to room temperature to brine.

X-Ray Diffraction Pattern

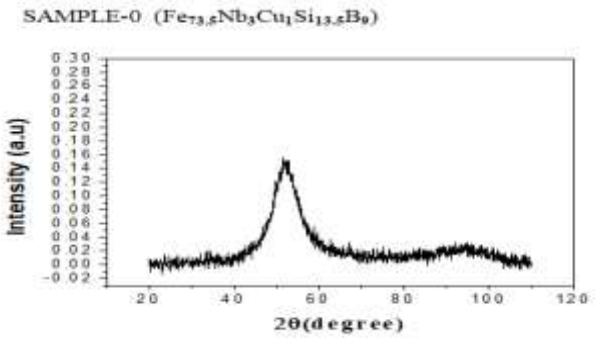

Figure 1.4.1: XRD of sample ($Fe_{73.5}Nb_3Cu_1Si_{13.5}B_9$)

ISSN No. 2454-6194 | DOI: 10.51584/IJRIAS |Volume XI Issue V May 2026

SAMPLE-1 ($Fe_{81}B_{12}Mo_7$)

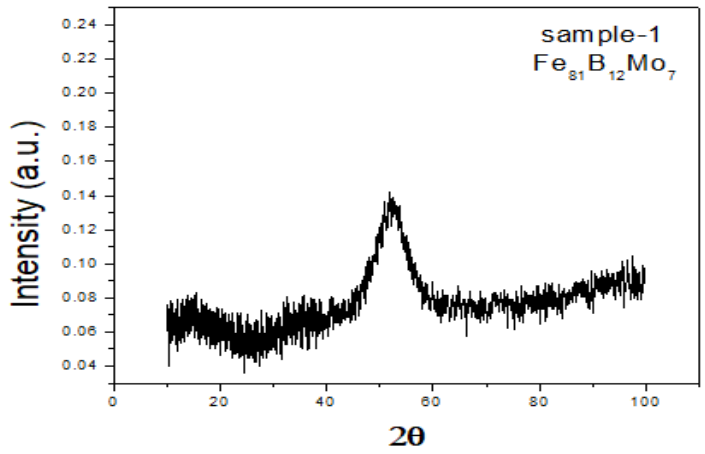

Figure 1.4.2: XRD of sample ($Fe_{81}B_{12}Mo_7$)

SAMPLE-2 ($Fe_{80}B_{12}Mo_7Cu_1$)

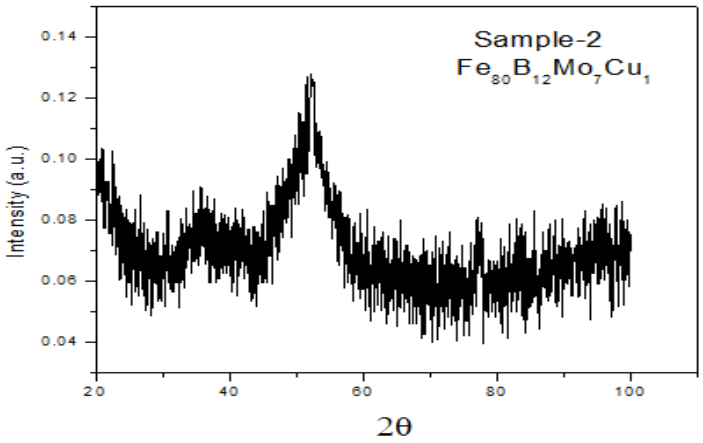

Figure 1.4.3: XRD of sample-2 ($Fe_{80}B_{12}Mo_7Cu_1$)

SAMPLE-4 ($Fe_{83}B_{12}Mo_5$)

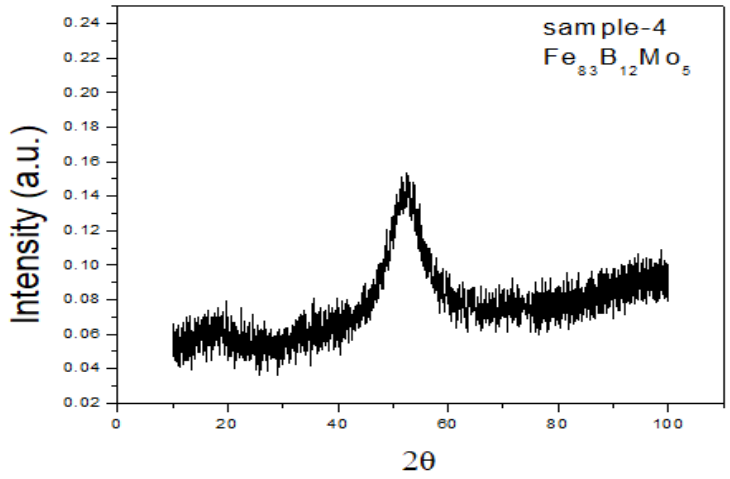

Figure 1.4.4: XRD of sample-4 ($Fe_{83}B_{12}Mo_5$)

ISSN No. 2454-6194 | DOI: 10.51584/IJRIAS |Volume XI Issue V May 2026

RESULTS AND DISCUSSION

The XRD pattern of the amorphous alloys FINEMET ($Fe_{73.5}Nb_3Cu1Si13.5B9$), SAMPLE-1 (Fe81B12Mo7), SAMPLE-2 (Fe80B12Mo7Cu1) & SAMPLE-4 (Fe83B12Mo5) are shown in above figure. The XRD pattern resembles that of a fully amorphous material, with a broad amorphous scattering maximum but no sharp diffraction features indicative of the presence of crystalline phase.

From the diffraction pattern we can see that there is a broad peak with a relatively very low intensity. The peak intensity of ~ 0.16 a.u for the amorphous metal is extremely small when compared to that for a crystalline substance where the peak intensity ranges up to some thousand a.u.

Also, we can see from the figure that the breadth of the peak is also very large. As shown in the Fig1.4.1, the peak has got a breadth of nearly 18 degrees (2d varies from nearly 42 to 60 degrees).

For the case of crystalline materials, the peak is extremely sharp i.e. the range of 2d is very small. Also, in the diffraction pattern we have obtained only one peak. If it had been for a crystalline material, then there would have been many more sharp peaks each resembling a lattice plane.

X-Ray diffraction pattern shows peak with high FWHM with a relatively very low intensity for all the samples [FINEMET ($Fe_{73.5}Nb_3Cu_1Si_{13.5}B_9$), SAMPLE-1 ($Fe_{81}B_{12}Mo_7$), SAMPLE-2 ($Fe_{80}B_{12}Mo_7Cu_1$), SAMPLE-3 ($Fe_{82}B_{12}Mo_7Cu_1$) and SAMPLE-4 ($Fe_{83}B_{12}Mo_5$)]. The peak intensity (~ 0.16 a.u.) for the amorphous metal is extremely small compared to that for a crystalline substance where the peak intensity ranges up to some thousand a.u. The XRD pattern resembles that the samples are fully amorphous material.

Fabrication of a low temperature T_C measurement set up

The set up basically uses a cryostat for cooling the sample and we can measure low temperature resistivity as well as Curie temperature (below room temperature) of a given sample using this set up. The important feature of the setup is that options are kept to mount at most four samples at a time for measurement. So far, we have completed necessary wirings of the set up such that we can do measurements of two samples simultaneously. Measurements of resistivity, Tc or both are possible at a time for the samples.

The Cryostat - The cryostat is made up of three chambers – a cylindrical sample chamber at the centre, a liquid nitrogen chamber coaxially covering the sample chamber and an outer chamber covering the liquid nitrogen chamber.

The vacuum ports- Two vacuum ports, one connected to the sample chamber and the other connected to the outer chamber are used for evacuation of the corresponding chambers.

The valves- Four valves are connected to the cryostat at different positions. Three of them are connected to the three chambers respectively. The flow Valve controls the flow of liquid nitrogen from liquid nitrogen chamber to the sample chamber.

ISSN No. 2454-6194 | DOI: 10.51584/IJRIAS |Volume XI Issue V May 2026

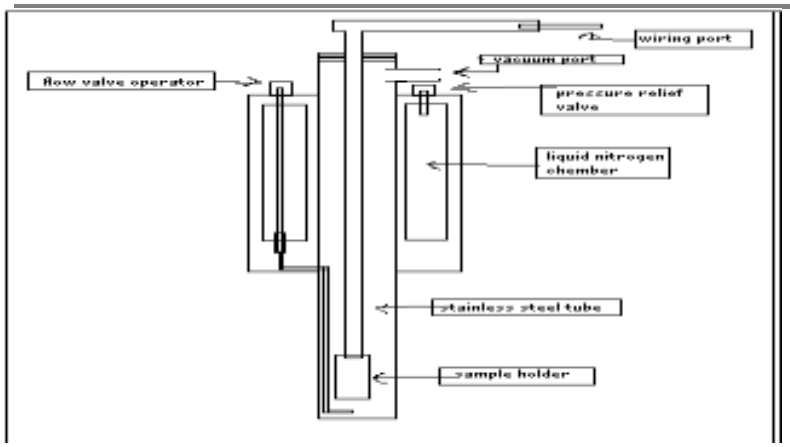

Figure1: Schematic diagram of the cryostat

The Sample Holder

The sample holder consists of two parts, one stainless steel tube and a copper block (1cm×1cm×9cm) as shown in Fig.2 (c)

a. The hollow tube is made of a non-magnetic material (stainless steel). All the connections are made through this tube. At one end of it a rubber tube is connected through which all connecting wires have emerged. The tube has been clamped to make it air tight.

b. The copper block (Fig.2 (a)) which contains the heater wire and the sensor is connected to the other end of the tube. Two grooves are created near the two extremes of the copper block for winding the heater wire. The platinum sensor is attached by a heat-conducting adhesive on 'C' side of the copper block. Half of the heater wire is wound non-inductively on the one groove and the rest of it is on the other.

Two insulating plates, each containing 10 thin copper strips parallel to each other and separated from each other by a small gap, are attached on both, "A" side and "B" side of the cooper block .

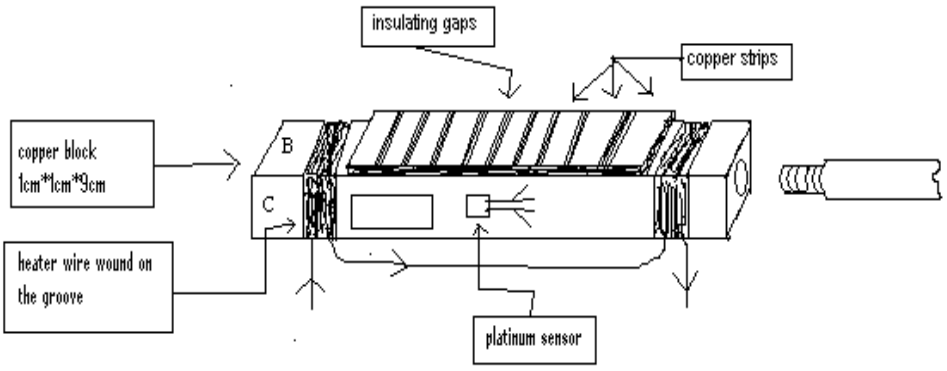

Figure .2 (a): Diagram of the sample holder (copper block)

ISSN No. 2454-6194 | DOI: 10.51584/IJRIAS |Volume XI Issue V May 2026

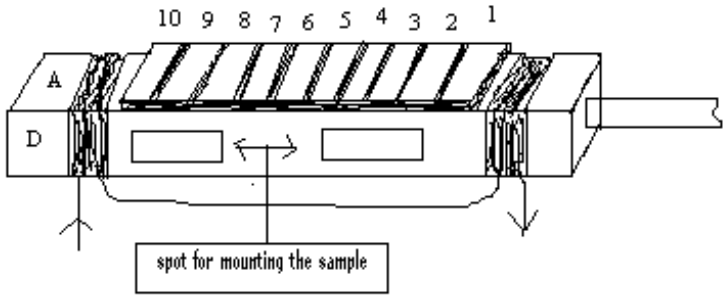

Figure .2 (b): Diagram of the sample holder (copper block)

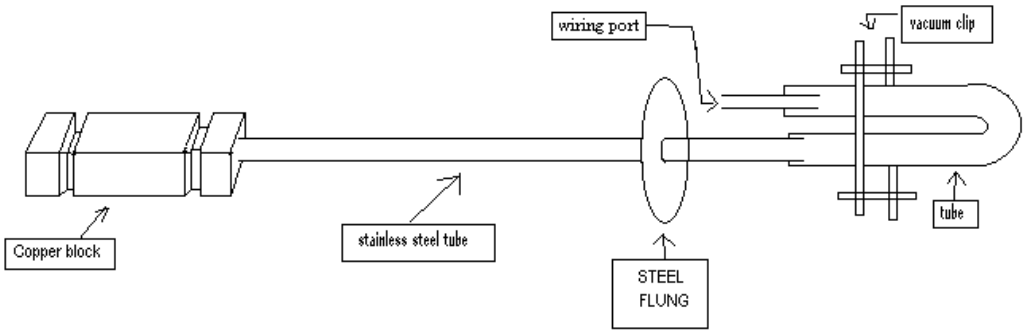

Figure .2 (c): Complete schematic diagram of the sample holder.

The Connections of the Wires.

A bunch of 24 insulating copper wires has been employed to make all the necessary connections. Sixteen of them are connected to the copper strips as shown in Fig.4.3 (a). Four wires have been used to make connection to the heater. Two connecting wires are connected to each of the heater wires. The two probes Platinum sensor has been converted into a four probe one by soldering two wires to each of the probes of the sensor. The terminal points of the 24 wires are connected to a 25-pin male connector socket as shown. The connections have been extended to a metal box by a female 25 pin socket to be connected to the previous one. In the metal box these wires are separated into two groups. Terminals of each group of wire are again connected to two 9 pin male sockets respectively. One of them contains all the wire terminals to be connected to the temperature controller. The other one should be connected to current source, LCR meter or voltmeter as per purpose.

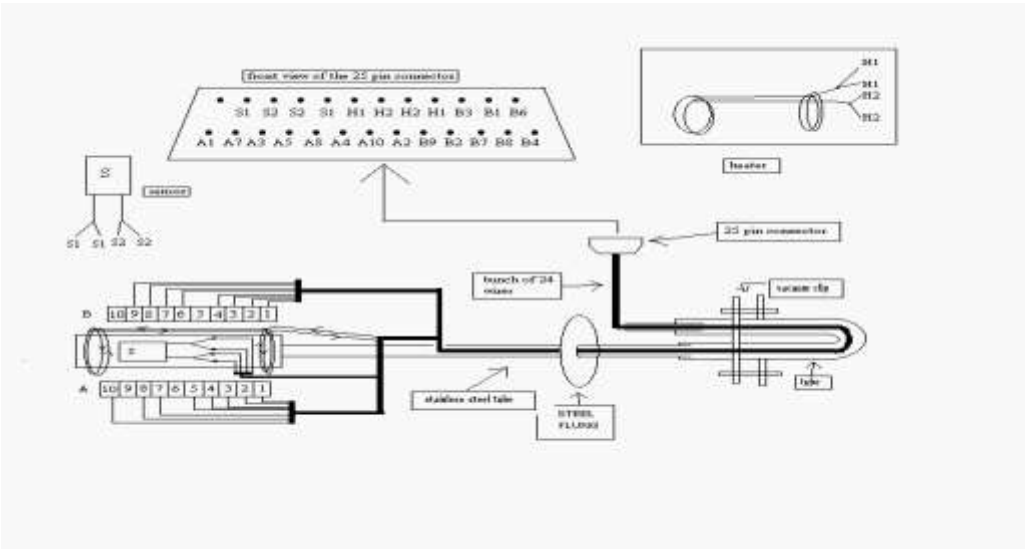

Figure3 :(a) Schematic diagram of the connections.

ISSN No. 2454-6194 | DOI: 10.51584/IJRIAS |Volume XI Issue V May 2026

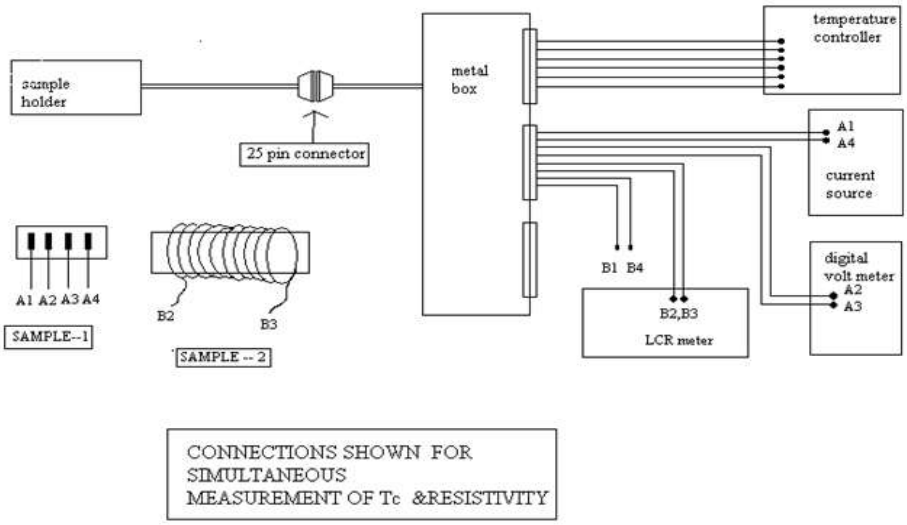

Figure .3 (b): Schematic diagram of the connections of the setup during measurement.

Sample mounting

A rectangular shaped sample is preferable for measurement of T_C of that sample. A 50-turn winding of enamelled copper wire is to be done on the middle of the sample as shown. Now using Teflon ties the sample at the copper block on its C or D side. The two ends of winding are soldered to B2 and B3 copper strips. Now this whole sample holder is to put into the cryostat.

Connections and measurement

The connection to the temperature controller is to be made as shown. The wires connected to B2 and B3 strips is to be joined to LCR meter as per diagram. Now the cryostat chambers should be evacuated using vacuum Pump and then liquid nitrogen is poured into the Nitrogen chamber to cool down the sample down to approximately 78 K. Now by using the temperature controller we can increase the temperature of the sample in a controlled manner. Now by switching on the LCR meter we can start taking readings of inductance at different temperatures. To calculate Tc we have to plot inductance as a function of temperature. We know the inductance of the coil with sample inside should be proportional to the permeability of the sample. So at Tc there will be a large drop in inductance around Tc. This Tc can be determined by looking at the derivative curve of the original curve which shows a minima at Tc.

Experimental results

Variation of inductance with temperature for sample-1($Fe_{81}B_{12}Mo_7$)

ISSN No. 2454-6194 | DOI: 10.51584/IJRIAS |Volume XI Issue V May 2026

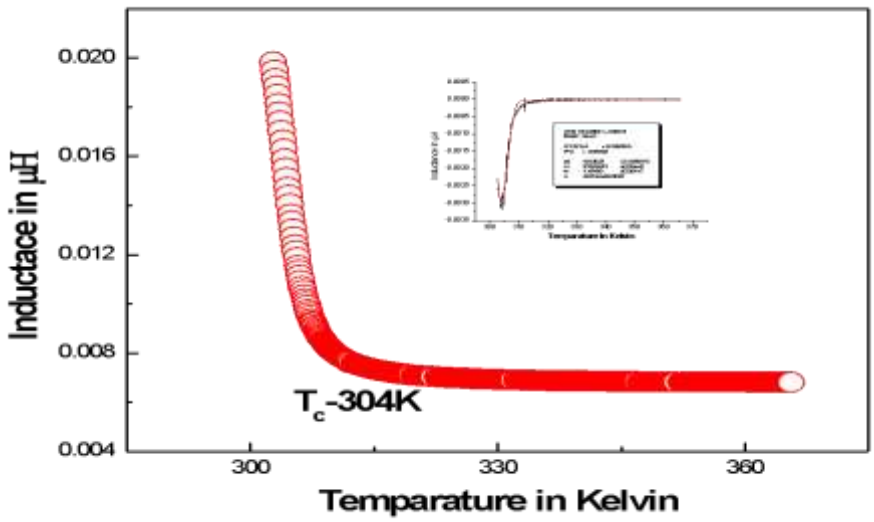

Figure 1.7: Inductance vs. temperature plot for sample-1($Fe_{81}B_{12}Mo_7$)

Variation of inductance with temperature for sample-2($Fe_{80}B_{12}Mo_7Cu_1$)

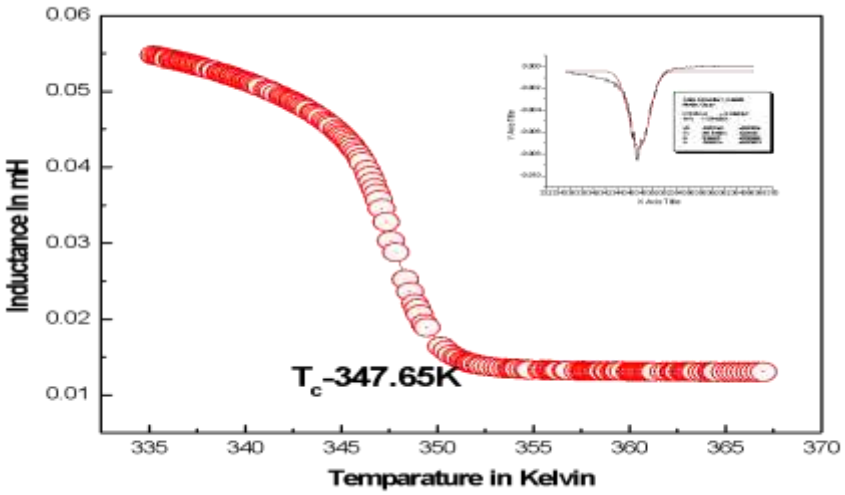

Figure.1.8: Inductance vs. temperature plot for sample-2($Fe_{80}B_{12}Mo_7Cu_1$)

DISCUSSION

Ferromagnetic to paramagnetic transition temperatures of all the metallic glasses samples have been measured by using the low temperature Tc measurement set up. To calculate curie temperature, inductance is plotted against temperature of the sample. Around Curie temperature inductance falls rapidly. Derivative of the curve shows a minimum exactly at the transition temperature. For the sample-1 Tc is 304 Kelvin (~ room temperature) and for the sample-2 the same is 347.65 Kelvin (above room temp.)

By identifying the minima (by Gaussian fit) Curie temperature has been calculated. It is very important to know the value of T_c because before doing any experiment it is significant to know the magnetic nature (FM or PM) of the sample. Moreover, the value of Tc gives us a measure of the ferromagnetic nature of the sample.

ACKNOWLEDGEMENT

ISSN No. 2454-6194 | DOI: 10.51584/IJRIAS |Volume XI Issue V May 2026

I want to acknowledge my project Supervisor Dr. Tapan Kumar Nath (Professor IIT- Kharagpur) for introducing me in Condensed matter physics. Also, I thankful to Prof. Sourav Marik for helping the experiments in the IIT-Kharagpur Lab.

I also express my deep gratitude to Mr. Anjan Mondal (Assistant teacher in physics), Mr. Somenath Chatterjee (Assistant Engineer in WBSETCL) and Parama Thakur (Astrologer) for their continuous help in the several stages of my work. They were always ready to help whenever I was doubt and clarify many of the experimental and basic concepts.

During this work I enjoy prompt physically help from Mr. K. Mallik. I extended him my sincere thanks.

Finally, I like to thank my friend Mr. Marik who worked with me jointly under the same supervisor, for his immense help and support during the conduct of my project.

REFERENCE

1. S Chattopadhyay, TK Nath ; Enhancement of room temperature ferromagnetism of Fe-doped ZnO emitaxial thin films with Al co-doping; Journal of Magnetism and magnetic Meterials,2011
2. SK Mandal, TK Nath; Temperature dependence of solubility limits of transition metals (Co, Mn, Fe and Ni) in ZnO nanoparticles; Applied physics letters,2006
3. S Mandal , J Panda, TK Nath ; Investigation of the critical behaviour and magnetocaloric effect in Y-Fe49Ni29Cr22 disordered austenitic stainless steel alloy by using the field dependence of magnetic entropy change; Journal of Alloys and compounds,2015
4. A Ahmad , AK Das; Size-dependent Structural and magnetic properties of disordered Co2FeAl Heusler alloy nanoparticles; Journal of Magnetism and Magnetic Materials,2019
5. A Sarkar, AK Das; Giant junction magnetoresistance effect in ferromagnet/semiconductor heterostructures; Journal of Applied Physics,2013
6. S Mandal , J Panda, TK Nath ; Investigation of the critical behaviour and magnetocaloric effect in Y-Fe49Ni29Cr22 disordered austenitic stainless steel alloy by using the field dependence of magnetic entropy change; Journal of Alloys and compounds,2015.
7. Ferromagnetism in Fe-doped ZnO nanocrystals: experiment and theory D Karmakar,SK Mandal, RM Kadam, PL Paulose, AK Rajarajan, TK Nath, Physical Review B 75 (14), 144404.
8. Electronic structure and magnetism of the diluted magnetic semiconductor Fe-doped ZnO nanoparticles T Kataoka, M Kobayashi, Y Sakamoto, GS Song, A Fujimori, FH Chang, Journal of Applied Physics 107 (3), 033718
9. Complex permeability and magnetization studies in some Fe-rich Soft ferro-magnetic Glasses. Prof. Debashis Das, Shpbpur Dinobundhoo Institution College.Journal of Neuro-Quantology , sept 2022, volume20, page 01-14, Issue-11.
10. Fabrication of High Temperature T_C measurement Set-up and to Study of GMI of some iron rich soft Ferromagnetic Materials. Prof. Debashis Das. Shpbpur Dinobundhoo Institution College. Journal of Neuro-Quantology , sept 2022, volume20, page 3119-3128, issue-9.